Journal of Visualized Experiments
Doxycycline Loaded Collagen-Chitosan Composite Scaffold for the Accelerated Healing of Diabetic Wounds
--Manuscript Draft--

Article Type:	Invited Methods Collection - Author Produced Video
Manuscript Number:	JoVE62184R4
Full Title:	Doxycycline Loaded Collagen-Chitosan Composite Scaffold for the Accelerated Healing of Diabetic Wounds
Corresponding Author:	Veera Venkata Satyanarayana Reddy Karri, M. Pharm., Ph.D. JSS College of Pharmacy Ooty Ooty, Tamil Nadu INDIA
Corresponding Author's Institution:	JSS College of Pharmacy Ooty
Corresponding Author E-Mail:	ksnreddy87@gmail.com
Order of Authors:	Bharat Kumar Reddy Sanapalli
	Kalaivani C
	Nilesh Sudhakar Ambhore
	Gowthamarajan Kuppuswamy
	Praveen TK
	Veera Venkata Satyanarayana Reddy Karri

Additional Information:	
Question	Response
Please indicate whether this article will be Standard Access or Open Access.	Standard Access (US$1200)
Please confirm that you have read and agree to the terms and conditions of the author license agreement that applies below:	I agree to the Author License Agreement
Please specify the section of the submitted manuscript.	Bioengineering
Please indicate whether this article will be Standard Access or Open Access.	Standard Access ($1400)
Please provide any comments to the journal here.	

Manuscript

Click here to access/download;Manuscript;62184_R4.docx ⬇

1 **TITLE:**
2 Doxycycline Loaded Collagen-Chitosan Composite Scaffold for the Accelerated Healing of
3 Diabetic Wounds
4
5 **AUTHORS AND AFFILIATIONS:**
6 Sanapalli Bharat Kumar Reddy[1], Chinna Gounder Kalaivani[1], Ambhore Nilesh Sudhakar[2],
7 Kuppuswamy Gowthamarajan[1], Thaggikuppe Krishnamurthy Praveen[3], Karri Veera Venkata
8 Satyanarayana Reddy[1]*
9
10 1.   Department of Pharmaceutics, JSS College of Pharmacy, JSS Academy of Higher Education
11 & Research, Ooty, Nilgiris, Tamilnadu, India
12 2.   Department of Pharmaceutical Sciences, School of Pharmacy, North Dakota state
13 university, Fargo, ND, USA
14 3.   Department of Pharmacology, JSS College of Pharmacy, JSS Academy of Higher Education
15 & Research, Ooty, Nilgiris, Tamilnadu, India
16
17 Email Address for co-authors
18 Bharat Kumar Reddy. Sanapalli   (bharathsanapalli@yahoo.in)
19 Kalaivani. Chinna Gounder   (kalai14795@gmail.com)
20 Nilesh Sudhakar. Ambhore   (nilesh2484@gmail.com)
21 Gowthamarajan. Kuppuswamy   (gowthamsang@jssuni.edu.in)
22 Praveen. Thaggikuppe Krishnamurthy   (praveentk7812@gmail.com)
23 Veera Venkata Satyanarayana Reddy. Karri   (ksnreddy87@gmail.com)
24
25 *Address for Correspondence:
26 Veera Venkata Satyanarayana Reddy Karri (ksnreddy87@gmail.com)
27
28 **KEYWORDS:**
29 Diabetic wound; Doxycycline; Collagen; Chitosan; Scaffold
30
31 **SUMMARY:**
32 The prepared DOX-CL scaffold satisfied the prerequisites of an ideal DW dressing in mechanical
33 strength, porosity, water absorption, degradation rate, sustained release, anti-bacterial,
34 biocompatibility, and anti-inflammatory properties, which are considered to be essential for the
35 recovery of damaged tissue in DWs.
36
37 **ABSTRACT:**
38 One major complication of diabetes mellitus is diabetic wounds (DW). The prolonged phase of
39 inflammation in diabetes obstructs the further stages of an injury leading to delayed wound
40 healing. We selected doxycycline (DOX), as a potential drug of choice, due to its anti-bacterial
41 properties along with its reported anti-inflammatory properties. The current study aims to
42 formulate DOX loaded collagen-chitosan non-crosslinked (NCL) & crosslinked (CL) scaffolds and
43 evaluate their healing ability in diabetic conditions. The characterization result of scaffolds
44 reveals that the DOX-CL scaffold holds ideal porosity, a low swelling & degradation rate, and a

45   sustained release of DOX compared to the DOX-NCL scaffold. The *in vitro* studies reveal that the
46   DOX-CL scaffold was biocompatible and enhanced cell growth compared with CL scaffold treated
47   and control groups. The anti-bacterial studies have shown that the DOX-CL scaffold was more
48   effective than the CL scaffold against the most common bacteria found in DW. Using the
49   streptozotocin and high-fat diet-induced DW model, a significantly ($p \leq 0.05$) faster rate of wound
50   contraction in the DOX-CL scaffold treated group was observed compared to those in CL scaffold
51   treated and control groups. The use of the DOX-CL scaffold can prove to be a promising approach
52   for local treatment for DWs.
53
54   **INTRODUCTION:**
55   Diabetes mellitus (DM) is a condition where the body's failure to deliver insulin or react to its
56   outcomes in abnormal digestion of straightforward sugars brings about an upsurge of blood
57   glucose [1]. The most consecutive and crushing entanglement of DM is the diabetic wound (DW).
58   Roughly 25% of patients with DM have the opportunity to build up a DW in their lifetime [1]. The
59   hindered healing of DW is accredited to a triopathy of DM: immunopathy, vasculopathy, and
60   neuropathy. Whenever DW is left untreated, it may result in gangrene development, therefore
61   prompting the removal of the concerned organ [2].
62
63   Plenty of treatments, such as instructing the patients (inspect wound daily, cleanse the wound,
64   avoid activities that creates pressure on the wound, periodic glucose monitoring, etc.),
65   controlling their blood glucose, wound debridement, pressure offloading, medical procedure,
66   hyperbaric oxygen therapy, and advanced therapies are in practice [3,4]. The majority of these
67   medications fail to address all prerequisites vital for DW care in light of the multifactorial
68   pathophysiological conditions and unexpected expenses related to these medicines [5]. Even
69   though the DW pathogenesis is multifactorial, the persistent inflammation with inappropriate
70   tissue management is stated to be the actual reason for delayed healing in DWs [5,6].
71
72   Augmented levels of inflammatory and pro-inflammatory mediators in DW result in diminished
73   growth factors responsible for delayed wound healing [2,6]. Improper extracellular matrix (ECM)
74   formation in DWs is accredited to increased levels of matrix metalloproteinases (MMPs)
75   accountable for the rapid degradation of formed ECM. In MMPs, MMP-9 is reported as a major
76   intermediary responsible for prolonged inflammation and rapid ECM degradation [7]. It is stated
77   that local treatment with an anti-inflammatory drug that decreases the elevated levels of MMP-
78   9 re-establishes cutaneous homeostasis, framework arrangement and prompts better healing of
79   DWs [8,9].
80
81   Doxycycline (DOX), an MMP-9 inhibitor, was chosen to suppress the elevated levels of MMP-9, a
82   major inflammatory mediator responsible for persistent inflammation in DWs [10-12]. In addition,
83   DOX possess antioxidant (produce free hydroxy and phenoxy radicals capable of binding with
84   reactive oxygen species) [13] and anti-apoptotic (inhibit caspase expression and mitochondrial
85   stabilization) [14] activities that are essential for the treatment of DW. The arrangement of
86   frameworks containing DOX, collagen (COL), and chitosan (CS) was chosen. The choice of COL
87   depends on the way that it helps in providing the necessary framework responsible for
88   mechanical strength and tissue regeneration [15]. On the other hand, CS is structurally homologous

89 to glycosaminoglycan, associated with several wound healing phases. It is also reported that CS
90 holds significant anti-bacterial property [15]. Hence, the COL/CS scaffold of DOX is formulated to
91 suppress the prolonged inflammation, followed by supporting the matrix formation for
92 successful wound healing in DM conditions.
93
94 **PROTOCOL:**
95
96 All the animal procedures performed were approved by the institutional animal ethical
97 committee of JSS College of Pharmacy, Ooty, India.
98
99 **1.   Preparation of DOX loaded porous scaffolds by freeze-drying method**
100
101 1.1.   Add 1.2 g of COL to 100 mL of water (e.g., Millipore) and keep aside for swelling.
102
103 1.2.   Stir the swollen COL dispersion at 2000 rpm overnight to ensure complete dissolution of
104 COL.
105
106 1.3.   Prepare CS solution by dissolving approximately 0.8 g of CS in 100 mL of 1% acetic acid.
107
108 1.4.   Stir the CS solution overnight at 2000 rpm to ensure uniform dispersion.
109
110 1.5.   Mix DOX (1 % w/v), followed by CS solution, to the COL solution, and stir for 30 min.
111
112 1.6.   Filter the obtained physical mixture using a muslin cloth to remove the particulate matter.
113
114 1.7.   Deep freeze the obtained filtrate at -85 °C ± 4 °C for about 24 h.
115
116 1.8.   Lyophilize the deep freeze mixture at -85 °C ± 4 °C for 72 h.
117
118 1.9.   Store the obtained scaffolds in a desiccator for further analysis [16,17].
119
120 **2.   Crosslinking of scaffold**
121
122 2.1.   Dissolve MES (0.488 g) in 50 mL of water.
123
124 2.2.   Soak 50 mg of the DOX loaded scaffold in 20 mL of the MES buffer for 30 min.
125
126 2.3.   Mix 19.5 mL of MES buffer with 0.1264 g of EDC and 0.014 g of NHS in a separate beaker.
127
128 2.4.   Immerse the scaffold in the buffer mixture for 4 h to achieve crosslinking [16].
129
130 2.5.   Store the DOX loaded crosslinked (CL) and non-crosslinked scaffolds (NCL) for further
131 evaluation.
132

3.   Characterization of scaffolds

3.1.   Morphological examination using a scanning electron microscopy (SEM)

3.1.1. Characterize the scaffolds for morphological analysis using SEM (1 cm × 1 cm × 0.5 cm).

3.1.2. Stain the cross-section and exterior surface of the scaffold with the delicate layer of gold (~150 Å).

3.1.3. Capture the photographic image at the excitation voltage of 5 kV and 10 kV.

3.1.4. Place the samples in aluminum stubs and enclose them with the gold at approximately 9 V.

3.1.5. Measure the scaffold using SEM with the increased resolution at 10 kV.

3.2.   Porosity determination

3.2.1. Measure the porosity of the scaffolds using the liquid displacement method (ethanol) [18].

3.2.2. Calculate the porosity of the scaffolds using the below formulae.

$$Porosity\ (\%) = \frac{Ww - Wd}{Wv} \times 100$$

W_w = Wet weight of the scaffold
W_d = Dry weight of the scaffold
W_v = Volume of the scaffold

3.3.   Determining the water absorption capacity

3.3.1. Measure the dry weight of the scaffold.

3.3.2. Incubate the weighed scaffold at 37 °C for 24 h in phosphate buffer saline (PBS) pH 7.4.

3.3.3. Remove the excess PBS over the scaffold using filter paper.

3.3.4. Measure the water absorption capacity using the below formulae [17].

$$WS\ \% = (W1 - W0)/W0$$

W_S = Percentage of water absorption
W_1=Wet weight of the scaffold
W_0= Dry weight of the scaffold

3.4.   Scaffold degradation

3.4.1. Incubate the scaffold (1cm x 1cm) at 37 °C for 7 days in a PBS of pH 7.4 containing

176   lysozymes.

177

178   3.4.2. Wash the scaffold to remove any adhered ions on the surface.

179

180   3.4.3. Freeze dry the washed scaffold [17].

181

182   3.4.4. Calculate the rate of degradation using formulae.

183

184    $$Degradation \% \ = \ \frac{[Ww - Wd]}{Ww} \times 100$$

185   Ww = Initial weight of the scaffold
186   Wd = Weight of the scaffold after freeze-drying

187

188   **3.5.   *In vitro* release studies**

189

190   3.5.1. Determine the release behavior of the DOX from the scaffold using the dialysis sack
191   method.

192

193   3.5.2. Disperse the scaffold in a few milliliters of simulated wound fluid (pH 7.4) and transfer it
194   into a dialysis bag.

195

196   3.5.3. Tightly close the ends of the membrane bag and immerse in the 500 mL of simulated
197   wound fluid solution.

198

199   3.5.4. Stir the wound fluid solution containing the dialysis bag at 200-250 rpm.

200

201   3.5.5. Collect the supernatant solution and replace it with an equal quantity of fresh buffer
202   solution at definite time intervals.

203

204   3.5.6. Determine the percentage of DOX release from the scaffolds in the supernatant solution
205   using a UV-visible spectrometer at 240 nm.

206

207   **4.   *In vitro* anti-bacterial studies**

208

209   4.1.   Determine the minimum inhibitory concentration (MIC) of the CL and DOX-CL scaffolds
210   against the *S. aureus*, *S. epidermis*, *E. coli*, *P. aeruginosa* using the micro-broth dilution method.

211

212   4.2.   Prepare the bacterial cultures using Mueller-Hinton broth at a ratio of 1:1000 to obtain
213   0.5 McFarland turbidity.

214

215   4.3.   Add D-glucose (800 mg/dL) to the bacterial cultures for hyperglycation [19,20].

216

217   4.4.   Mince and solubilize the CL and DOX-CL in DMSO (negative control).

218

219   4.5.   Serially dilute the hyperglycated bacterial suspension (100 µL) and test samples (100 µL
220   of scaffolds solution) in 96 well plate.
221
222   4.6.   Incubate the plate at 37 °C for 20-24 h.
223
224   4.7.   Record the absorbance at a wavelength of 600 nm [21].
225
226   **5.**   ***In vitro* biocompatibility studies**
227
228   5.1.   Evaluate the biocompatibility of the prepared scaffolds using MTT [(3-(4, 5 dimethyl
229   thiazole-2 yl) -2, 5-diphenyl tetrazolium bromide)] assay.
230
231   5.2. Sterilize the scaffolds of standard dimension and place them in 24 well plates.
232
233   5.3. Add 3T3-L1 cells to the 24 well plate and incubated for 72 h.
234
235   **6. *In vivo* animal studies**
236
237   **6.1. Induction of DM and excision wound**
238
239   6.1.1. Feed the animal with a high-fat diet for two weeks and administer a single dose of
240   streptozotocin (STZ) (50 mg/kg body weight) in citrate buffer solution intraperitoneally to Wistar
241   albino rats (180-200 g) for the induction of type-2 diabetes.
242
243   6.1.2. Choose the animals with a constant blood glucose of 250 mg/dL for the study.
244
245   6.1.3. Randomize the selected animals for the induction of excision wounds.
246
247   6.1.4. Anesthetize the diabetic rats using diethyl ether (5 mL was added to the priorly saturated
248   anesthesia chamber) and confirm using the toe pinch method and mucous membrane color.
249
250   6.1.5. Shave the dorsal area (Dorsal thoracic, lumbar region) using an aseptic trimmer and blades
251   (A40).
252
253   6.1.6. Sterilize the shaved area with an alcoholic swab.
254
255   6.1.7. Excise the skin (2 x 2 cm^2 and a depth of 1 mm) with an aseptic surgical A40 blade on the
256   shaved area to create an open wound.
257
258   6.1.8. Divide the animals into three groups (Group 1- Disease control (Control), Group 2- CL
259   scaffold (Placebo), Group 3- DOX CL scaffold), each group consisting of 6 rats.
260
261   6.1.9. Affix the CL and DOX CL scaffolds using surgical tape and cover the control group with
262   sterile gauze for 21 days.

263

264 6.1.10. Trace the wound area on a sterile OHP sheet and measure the percentage reduction of
265 the wound using the grid method on days 0, 7, 14, and 21 for all groups.

266

267 6.1.11. Calculate the percentage wound reduction using the below formulae.

268 $$\% \, wound \, contraction = \frac{wound \, area \, on \, day \, 0 - wound \, area \, on \, a \, particular \, day}{wound \, area \, on \, day \, 0} x100$$

269

270 **7.   Histopathological studies**

271

272 7.1.   Isolate the healed wound area on days 7, 14, and 21, store in formalin solution (10%).

273

274 7.2.   Section the tissues using a microtome to obtain a thickness of 6 μm.

275

276 7.3.   Mount the sections on a glass slide and stain using Hematoxylin and eosin [17].

277

278 7.4.   Capture the images under 40x magnification using a digital microscope.

279

280 **8.   Hydroxyproline estimation**

281

282 8.1.   Isolate the healed wound area on days 0, 7, 14, and 21 for evaluation.

283

284 8.2.   Estimate the hydroxyproline content using the procedure described by Reddy G et al.,
285 1996 [22].

286

287 **9.   Elisa test**

288

289 9.1. Estimate the MMP-9 levels using the Elisa kit as per the manufacturer's instructions.

290

291 9.2. Isolate the tissue samples from the healed wound area on day 21 and mince using a tissue
292 homogenizer.

293

294 9.3. Centrifuge the obtained homogenate and collect the supernatant.

295

296 9.4. Dilute the supernatant at 100-fold using assay buffer.

297

298 9.5. Scan the plate using a multiple plate reader.

299

300 **10.   Statistical analysis**

301

302 10.1. Represent the obtained outcomes as Mean ± SD.

303

304 10.2. Perform the statistical analysis using Graph pad prism v5.01.

305

306 10.3. Attain the statistical significance using One Way Analysis of Variance (ANOVA) and Dunnet's
307 post hoc test.

308

309 10.4. Consider the values with p≤0.05 as significant.

310

311 **REPRESENTATIVE RESULTS:**
312 **Characterization of the DOX loaded NCL and CL scaffold**
313 On visual examination, the NCL and CL scaffold was found to be cream in color. Besides, both the
314 scaffolds appear to be like a sponge, stiff and inelastic when examined physically. SEM images of
315 the NCL and CL scaffolds are shown in **Figure 1**. From the figure, it was clear that there was a
316 decrease in pore size after crosslinking by forming intermolecular linkages. Also, the NCL and CL
317 scaffolds porosity were found to be 92.3±4.21 and 71.35±2.65, respectively. The percentage of
318 water absorption of the NCL and CL scaffolds was 750±11.4% and 492±8.66% at 24 h time
319 intervals.

320

321 In addition, biodegradation studies were performed for seven days in the simulated wound fluid
322 of pH 7.4, comprising lysozymes. The NCL scaffold exhibited a faster rate of degradation initially
323 in the first three days and decreased slowly for four consecutive days. On the other side, the CL
324 scaffold showed a prolonged rate of degradation. Crosslinking of the scaffold enhanced
325 mechanical properties and network strength that, in turn, resulted in decreased degradation
326 rate, indicating improved resistance to the degradation (**Figure 2**).

327

328 Further, the *in vitro* release of DOX from NCL and CL scaffold was performed for 120 h (**Figure 3**).
329 In the initial 1 h, 27.92±3.45% DOX was released from the NCL scaffold, whereas only
330 16.54±2.21% DOX was released from the CL scaffold. After 6 h, the DOX release from the scaffolds
331 increased by 63.15±3.78% in the NCL scaffold and 44.43±3.57% in CL scaffolds. After 24 h, there
332 was a release of 70% DOX from the NCL scaffold, whereas CL scaffold took more than 72 h to
333 release 70% of the DOX. Based on the results obtained, the DOX loaded CL scaffold was selected
334 for further evaluation and represented as DOX-CL Scaffold. Whereas CL scaffold without DOX
335 (placebo) is designated as CL Scaffold.

336

337 ***In vitro* anti-bacterial studies**
338 Patients with DW usually experience infections that result in prolonged wound healing. Thus,
339 prepared scaffolds were examined for their anti-bacterial activity using the MIC against a selected
340 panel of bacteria (**Table 1**). From the results, it is clear that DOX exhibited inhibitory activity with
341 a MIC of <4 µg/mL against both *S. aureus* and *S. epidermis.* A MIC of <8 µg/mL and <16 µg/mL
342 was observed against *E. coli* and *P. aeruginosa*. Alone chitosan and CL scaffold extract exhibited
343 minimal activity against selected organisms such as *S. aureus* (<64 µg/mL), *S. epidermis* (<64
344 µg/mL), *E. coli* (<128 µg/mL), and *P. aeruginosa* (<128 µg/mL). DOX-CL scaffold has shown similar
345 inhibitory activity with a MIC of <2 µg/mL against both *S. aureus* and *S. epidermis*. Further, the
346 DOX-CL scaffold exhibited moderate activities with a MIC of <8 µg/mL against E. coli and P.
347 aeruginosa.

348

349 ***In vitro* biocompatibility study**

MTT assay was performed to determine the cellular viability of 3T3-L1 cells in the presence of CL and DOX-CL scaffolds. The results exemplified that the CL and DOX-CL scaffolds did not stimulate any cytotoxicity. Furthermore, the cellular viability was comparatively higher in the scaffold treated groups than in control, representing the enhanced growth of fibroblasts in the presence of scaffolds (**Figure 4**).

In vivo wound healing studies

The mean wound area decreased in all the groups was determined using the graphical method on days 0, 7, 14, and 21 (**Figure 5**). On visual examination, the wounds in the CL and DOX-CL scaffold treated groups were free from oozing on day seventh. At the same time, the wounds in the control group were oozing. On day 14, a dry scab was observed in all groups; however, a faster rate of wound contraction was observed in the DOX-CL scaffold (89.663%). On day 21, 99.9% of the wound got healed, and a scar was formed in the DOX-CL scaffold, whereas partial healing was observed in control and CL scaffold treated groups.

Histopathology study

Histopathological observation of wound healing on day seventh postinjury exhibited disruption of all skin layers at the edges of the wound in all groups. There was no visibility of the epidermis; however, predominant neutrophils with intermittent monocytes and lymphocytes were observed in the control group. In CL scaffold treated group, moderate visibility of epidermis was noticed along with few neutrophils and macrophages. Whereas, in the DOX-CL scaffold treated group, the wound was covered with a slim layer of the epidermis, representing the phase of reepithelization. Mild neutrophils and macrophages, along with granulation tissue, were also seen more often in the DOX-CL scaffold treated group.

On day 14 postinjury, wounds in all the groups were found to be covered with epidermis. In the control group, the epidermis layer formed was observed to be a very slim layer along with prevailed neutrophils. In the CL scaffold treated group, the epidermis layer formed was thicker than that in the control group, along with mild multinucleated massive cells. In the DOX-CL scaffold treated group, the epidermis developed was thicker compared to other groups, along with an abundant number of histiocytes and giant multinucleated cells. The dense zone of fibroblasts was also observed in the DOX-CL scaffold treated group.

On day 21 postinjury, in the control group, a dominant number of neutrophils were decreased along with recurrence of macrophages and histiocytes representing the decreased inflammation. Whereas, in the CL scaffold treated group, a moderate number of histocytes and lymphocytes were observed. The epidermis formed was observed to be substantially thicker in the DOX-CL scaffold treated group than those in the control group, along with a rich number of histiocytes, lymphocytes, and massive multinucleated cells. In the DOX-CL scaffold treated group, the neutrophils count was decreased on day 7. Also, the gathering of macrophages and their morphological variants such as multinucleated massive cells and histiocytes were noticed on day 14 and 21 (**Figure 6**).

Hydroxyproline estimation

Hydroxyproline estimation is an indirect measure of the amount of collagen present in healing wounds. Higher hydroxyproline concentration designates a rapid percentage of wound healing. The biochemical examination revealed a higher amount of hydroxyproline in the DOX-CL scaffold treated group followed by the CL scaffold treated group than those in the control group (**Figure 7**).

MMP-9 estimation using the Elisa kit
MMP-9 content in the DOX-CL scaffold treated group was significantly decreased compared to those in control, and CL scaffold treated group. Whereas the MMP-9 content in the CL scaffold treated group was marginally less compared with that of the DOX-CL scaffold treated group, as shown in **Figure 8**.

FIGURE AND TABLE LEGENDS:
Figure 1: Morphology of DOX loaded COL-CS scaffold **a**) before CL and **b**) after CL determination by SEM at a scale range of 50 μm.

Figure 2: Matrix degradation of DOX loaded in NCL and CL scaffolds from day 1 to 7 in PBS pH 7.4 at 37 °C showing NCL degraded gradually for 7 days. Contrary to this, the CL scaffold degradation rate reduced considerably indicates enhanced resistance to enzymatic degradation.

Figure 3: In vitro drug release profile of DOX from NCL and CL scaffolds in PBS pH 7.4 at 37° C showing a slow release of drug in all formulation followed by a sustained release. Data expressed as mean ± SD (n=3).

Figure 4: 3T3-L1 cells cultured in the presence of CL and DOX-CL scaffolds showing percentage cell growth more in DOX-CL scaffold treated group followed by CL scaffold treated and control.

Figure 5: (**a**) Images representing the reduction in mean wound area in the control, CL scaffold and DOX-CL scaffold treated groups on day 0, 7, 14 and 21 post wounding. (**b**) Graphical representation of reduction in mean wound area in the control, CL scaffold and DOX-CL scaffold treated groups on day 0, 7, 14 and 21 post wounding. Data is expressed as mean ± SD (n=6 wounds/ group). Statistical significance was obtained by One Way Analysis of Variance (ANOVA) followed by Dunnet's post hoc test.

Figure 6: Histological changes during the wound healing process in STZ and high-fat diet-induced induced diabetes in Wistar albino rat skin on days 7, 14, and 21 without (control) and with treatment (CL and DOX-CL scaffolds) in a full-thickness excision wound model.

Figure 7: Result representing the hydroxyproline content in wounds on days 0, 7, 14, and 21 as an indicator of indirect collagen level estimation. The results are expressed in μg hydroxyproline/ mg of dry wound tissue. The data represents the Mean±SD (n=6 wounds/group). Statistical significance was obtained by One Way Analysis of Variance (ANOVA) followed by Dunnet's post hoc test.

438   **Figure 8**: Graph representing the MMP-9 levels in homogenates obtained from healed wounds
439   in STZ and high-fat diet-induced induced diabetic rat model on day 21. Levels of MMP-9 were
440   determined in 100-fold aliquots of wound fluids using ELISA analysis. The data represent
441   Mean±SD (n=3).

442

443   **Table 1**: Minimum inhibitory concentration of CS, DOX, CL, and DOX-CL Scaffolds against a
444   selected panel of bacteria.

445

446   **DISCUSSION:**
447   The main objective of this study was to determine the effect of DOX loaded COL-CS scaffold on
448   DW healing in rats. CL and NCL were prepared and evaluated in terms of morphology, swelling
449   index, in vitro release kinetics, and biocompatibility.

450

451   **Characterization of the DOX loaded NCL and CL scaffold**
452   The prepared scaffolds were found to be porous with interconnected pores. These
453   interconnected pores assure the porous, spongy nature that helps in the proper diffusion of
454   oxygen and nutrients to the cells for proliferation and migration, leading to accelerated healing.
455   Here, the pore size was mainly dependent on the crosslinking. Crosslinking the scaffold resulted
456   in decreased pore size by forming strong intramolecular interactions by EDC/NHS with CS and
457   COL, increasing the scaffold mechanical strength.

458

459   The porosity index relies on relative density, which is a function of the mass of sponge struts and
460   volume. Generally, shrinkage of scaffold volume occurs if a crosslinking agent alters the struts
461   position by dragging them closer to each other, leading to scaffold densification. However, in the
462   case of carbodiimide chemistry, an increase in the mass of scaffold is not anticipated due to its
463   unique mechanism, i.e., the introduction of amide linkage (O=C-NH) using carboxylic (>COOH)
464   and amine (-NH) group of adjacent peptide chain without entering into the scaffold.
465   Simultaneously, during crosslinking, minor mass loss may occur due to the dissolution and
466   migration of unattached polymer chains. Nevertheless, in case of scaffold treatment with
467   EDC/NHS did not produce any noticeable effect on scaffold morphology.

468

469   The ability of the scaffold to absorb biological fluid is crucial in evaluating its suitability as a drug
470   carrier. The water absorption property not only impacts the shape of the scaffold but also affects
471   cell growth. It was observed that the CL scaffold had shown a lower water absorption rate than
472   the NCL scaffold, which may be attributed to the crosslinking of the scaffold. Moreover, the
473   hydrophilicity of scaffold material was significantly reduced after crosslinking due to (i) loss of
474   hydrophilic groups (>COOH & -NH) in the process of amide linkage formation; (ii) inhibition of
475   swelling by the formation of new bonds (O=C-NH). These results are in good agreement with the
476   previously published reports [23,24].

477

478   An enzymatic biodegradation study was performed by monitoring the percentage of a residual
479   mass after seven days of incubation in the simulated wound fluid of pH 7.4, comprising
480   lysozymes. The NCL scaffold showed a faster rate of degradation initially in the first three days
481   and decreased slowly for four consecutive days. On the other side, the CL scaffold displayed a

482 prolonged rate of degradation. Crosslinking of the scaffold enhanced mechanical properties and
483 network strength that, in turn, resulted in decreased degradation rate, demonstrating improved
484 resistance to the degradation.
485
486 Drug release studies were performed for CL and NCL scaffolds for 120 h. In general, the scaffold's
487 drug release coefficient decreases as the crosslinking density increases due to enhanced
488 interconnections between the pores and decreased space between polypeptide chains. The drug
489 release coefficient is also influenced by the porosity index, water content, swelling index, and
490 degree of crosslinking. In our study, 27.92±3.45% and 63.15±3.78% of DOX from the NCL scaffold,
491 whereas 16.54±2.21% and 44.43±3.57% of DOX from the CL scaffold was released at 1 h and 6 h,
492 respectively. After 24 h, there was a release of 70% of DOX from the NCL scaffold, whereas; CL
493 scaffold took more than 72 h to release 70% of the DOX. The results showed that the scaffold
494 crosslinking inversely influenced DOX release by decreasing the swelling ratio and water content.
495
496 **_In vitro_ anti-bacterial studies**
497 DOX-CL scaffold extract exhibited higher inhibitory activity (MIC) against gram-positive
498 organisms. The higher activity of the DOX-CL scaffold extract might be because of the increased
499 hydrophobicity of the sample. However, DOX-CL scaffold extract exhibited minimal activity
500 against gram-negative organisms, probably due to cell wall penetration failure. Further, the MIC
501 of DOX-CL was comparatively higher than CS, CL scaffold, and DOX samples, which may be
502 attributed to the synergistic activity of DOX and CS in the DOX-CL extract.
503
504 **_In vitro_ biocompatibility study**
505 The _in vitro_ biocompatibility study was performed on fibroblast cells (3T3-L1). Fibroblasts are
506 responsible for the production of ECM and proteins. Further, they play a crucial role in
507 maintaining structural integrity by enhancing the formation of the framework required for
508 wound healing. The results show that the DOX-CL scaffold and CL scaffold did not produce any
509 cell cytotoxicity. However, both the scaffold groups were observed with the cell growth and
510 differentiation of fibroblasts in the scaffold pores, indicating that the prepared scaffolds were
511 biocompatible. Increased cell growth and differentiation in both the groups were mainly due to
512 the presence of CS and COL as an extracellular matrix in the scaffold structure.
513
514 Moreover, comparatively higher cell growth was observed with the DOX-CL scaffold group than
515 that of the CL scaffold due to activation of the PI3K-AKT signal by DOX, responsible for cell growth
516 and survival [25].
517
518 **_In vivo_ wound healing studies**
519 The various complications of DM are responsible for the prolonged healing of DW. To mimic the
520 diabetic condition in rats, a high-fat diet was given, followed by an intraperitoneal injection of
521 STZ. After 2-3 days of diabetic confirmation, open wounds were created by the excision of skin
522 at the dorsal thoracic region. The treatment was carried out for 21 days with respective scaffolds.
523 Reduction in the wound area was determined for all the groups on days 0, 7, 14, and 21. Diabetic
524 rats treated with the DOX-CL scaffold exhibited a significant degree of wound contraction
525 compared to CL scaffold groups and untreated groups.

526
527 The inflammatory phase of wound healing is responsible for functional barrier formation. In the
528 next stage, the proliferative phase of wound healing grabs attention in wound care, in which 43%
529 of wound area reduction was observed with the DOX-CL scaffold group. In comparison, only 23%
530 and 7% were observed with CL scaffold and untreated groups on day 7, respectively. From the
531 images (**Figure 5**), the contraction of the wound was initiated after the inflammatory and
532 proliferative phase completes. DOX-CL scaffold group exhibited significant wound contraction
533 due to the presence of DOX, which is responsible for the anti-inflammatory and anti-infective
534 effects. Moreover, COL and CS in the scaffold helped cell proliferation, differentiation, and
535 migration resulting in 99% of DW healing in 21 days.

536

537 Untreated excisional wounds showed neutrophils, lymphocytes, and monocytes on day 7
538 postinjury. As stated earlier, neutrophils aid in wound debridement in the early stage of wound
539 healing. Besides, the overabundance of neutrophils may negatively influence the healing process
540 by damaging the normal tissue. As reported by Dovi et al., a minimal number of neutrophils
541 accelerates the re-epithelialization process [26].

542

543 Further, increased macrophages, histiocytes, and massive multinucleated cells in the DOX-CL
544 scaffold treated group favored the environment for accelerated wound healing by repairing the
545 damaged cells and promoting the COL synthesis. Moreover, COL amalgamation with tissue was
546 determined using the hydroxyproline levels in all the groups. However, comparatively higher
547 hydroxyproline levels were observed with the DOX-CL scaffold treated group than the untreated
548 and CL scaffold treated group. As stated in the literature, the prolonged inflammatory phase in
549 the diabetic condition hinders the other phases of healing. The faster rate of wound contraction
550 in the DOX-CL scaffold may be attributed to DOX's anti-inflammatory property, resulting in the
551 further stages of the wound occurring in the proper time phase leading to accelerated wound
552 healing.

553

554 The biochemical estimation of MMP-9 levels using the ELISA test reveals that the DOX-CL scaffold
555 treated group exhibited decreased levels of MMP-9 in comparison with those in CL scaffold
556 treated and untreated groups. According to the literature, increased levels of MMP-9 responsible
557 for matrix degradation, which, in turn, prolongs the wound healing process. DOX, an anti-
558 inflammatory agent, inhibited the MMP-9 levels, which is considered the reason to prevent the
559 COL breakdown, resulting in accelerated DW healing. These results are in agreement with earlier
560 published studies by Lindeman et al., 2009 and Zhang et al., 2014 [27,28].

561

576 **DISCLOSURES:**
577 The authors declare that they have no competing financial interests.
578

579 **REFERENCES:**
580 1   International Diabetes Federation. IDF Diabetes Atlas, 9th edn. Brussels, Belgium: 2019.
581 Available at: https://www.diabetesatlas.org.
582 2   Falanga, V. Wound healing and its impairment in the diabetic foot. *The Lancet.* **366** (9498),
583 1736-1743 (2005).
584 3   Frykberg, R.G., Banks, J. Challenges in the treatment of chronic wounds. *Advances in
585 Wound Care*. **4** (9), 560-582 (2015).
586 4   Alexiadou, K., Doupis, J. Management of diabetic foot ulcers. *Diabetes Therapy.* **3** (1), 1-
587 15 (2012).
588 5   Karri, V. V. S. R. *et al.* Current and emerging therapies in the management of diabetic foot
589 ulcers. *Current Medical Research and Opinion.* **32** (3), 519-542 (2016).
590 6   Sanapalli, B. K. *et al.* Human beta defensins may be a multifactorial modulator in the
591 management of diabetic wound. *Wound Repair and Regeneration.* **28** (3), 416-421 (2020).
592 7   Caley, M. P., Martins, V. L., O'Toole, E. A. Metalloproteinases and wound healing.
593 *Advances in Wound Care.* **4** (4), 225-234 (2015).
594 8   Reiss, M. J. *et al.* Matrix metalloproteinase-9 delays wound healing in a murine wound
595 model. *Surgery.* **147** (2), 295-302 (2010).
596 9   Gill, S. E., Parks, W. C. Metalloproteinases and their inhibitors: regulators of wound
597 healing. *The International Journal of Biochemistry & Cell Biology.* **40** (6-7), 1334-1347 (2008).
598 10   Stechmiller, J., Cowan, L., Schultz, G. The role of doxycycline as a matrix metalloproteinase
599 inhibitor for the treatment of chronic wounds. *Biological Research for Nursing.* **11** (4), 336-344
600 (2010).
601 11   Griffin, M. O., Fricovsky, E., Ceballos, G., Villarreal, F. Tetracyclines: a pleitropic family of
602 compounds with promising therapeutic properties. Review of the literature. *American Journal of
603 Physiology-Cell Physiology.* **299** (3), C539-C548 (2010).
604 12   Burns, F., Stack, M., Gray, R., Paterson, C. Inhibition of purified collagenase from alkali-
605 burned rabbit corneas. *Investigative Ophthalmology & Visual Science.* **30** (7), 1569-1575 (1989).
606 13   Kraus, R. L. *et al.* Antioxidant properties of minocycline: neuroprotection in an oxidative
607 stress assay and direct radical-scavenging activity. *Journal of Neurochemistry.* **94** (3), 819-827
608 (2005).
609 14   Yrjänheikki, J., Keinänen, R., Pellikka, M., Hökfelt, T., Koistinaho, J. Tetracyclines inhibit
610 microglial activation and are neuroprotective in global brain ischemia. *Proceedings of the
611 National Academy of Sciences.* **95** (26), 15769-15774 (1998).

612 15   Moura, L. I., Dias, A. M., Carvalho, E., de Sousa, H. C. Recent advances on the development
613 of wound dressings for diabetic foot ulcer treatment—a review. *Acta Biomaterialia.* **9** (7), 7093-
614 7114 (2013).
615 16   Natarajan, J. *et al.* Nanostructured Lipid Carriers of Pioglitazone Loaded
616 Collagen/Chitosan Composite Scaffold for Diabetic Wound Healing. *Advances in Wound Care.* **8**
617 (10), 499-513 (2019).
618 17   Karri, V. V. S. R. *et al.* Curcumin loaded chitosan nanoparticles impregnated into collagen-
619 alginate scaffolds for diabetic wound healing. *International Journal Of Biological*
620 *Macromolecules.* **93** (Part B) 1519-1529 (2016).
621 18   Hsieh, W.-C., Chang, C.-P., Lin, S.-M. Morphology and characterization of 3D micro-porous
622 structured chitosan scaffolds for tissue engineering. *Colloids and Surfaces B: Biointerfaces.* **57** (2),
623 250-255 (2007).
624 19   Xie, Y., Chen, J., Xiao, A., Liu, L. Antibacterial activity of polyphenols: structure-activity
625 relationship and influence of hyperglycemic condition. *Molecules.* **22** (1913), 1-11 (2017).
626 20   Geerlings, S. E., Brouwer, E. C., Gaastra, W., Verhoef, J., Hoepelman, A. I. Effect of glucose
627 and pH on uropathogenic and non-uropathogenic Escherichia coli: studies with urine from
628 diabetic and non-diabetic individuals. *Journal of Medical Microbiology.* **48** (6), 535-539 (1999).
629 21   Eloff, J. N. A sensitive and quick microplate method to determine the minimal inhibitory
630 concentration of plant extracts for bacteria. *Planta Medica.* **64** (8), 711-713 (1998).
631 22   Reddy, G. K., Enwemeka, C. S. A simplified method for the analysis of hydroxyproline in
632 biological tissues. *Clinical Biochemistry.* **29** (3), 225-229 (1996).
633 23   Charulatha, V., Rajaram, A. Influence of different crosslinking treatments on the physical
634 properties of collagen membranes. *Biomaterials.* **24** (5), 759-767 (2003).
635 24   Rehakova, M., Bakoš, D., Vizarova, K., Soldán, M., Juríčková, M. Properties of collagen
636 and hyaluronic acid composite materials and their modification by chemical crosslinking. *Journal*
637 *of Biomedical Materials Research: An Official Journal of The Society for Biomaterials and The*
638 *Japanese Society for Biomaterials.* **30** (3), 369-372 (1996).
639 25   Chang, M.-Y. *et al.* Doxycycline enhances survival and self-renewal of human pluripotent
640 stem cells. *Stem Cell Reports.* **3** (2), 353-364 (2014).
641 26   Dovi, J. V., He, L. K., DiPietro, L. A. Accelerated wound closure in neutrophil-depleted mice.
642 *Journal of Leukocyte Biology.* **73** (4), 448-455 (2003).
643 27   Lindeman, J. H., Abdul-Hussien, H., van Bockel, J. H., Wolterbeek, R., Kleemann, R. Clinical
644 Perspective. *Circulation.* **119** (16), 2209-2216 (2009).
645 28   Zhang, C., Gong, W., Liu, H., Guo, Z., Ge, S. Inhibition of matrix metalloproteinase-9 with
646 low-dose doxycycline reduces acute lung injury induced by cardiopulmonary bypass.
647 *International Journal Of Clinical And Experimental Medicine.* **7** (12), 4975-4982 (2014).

Figure 1

1a
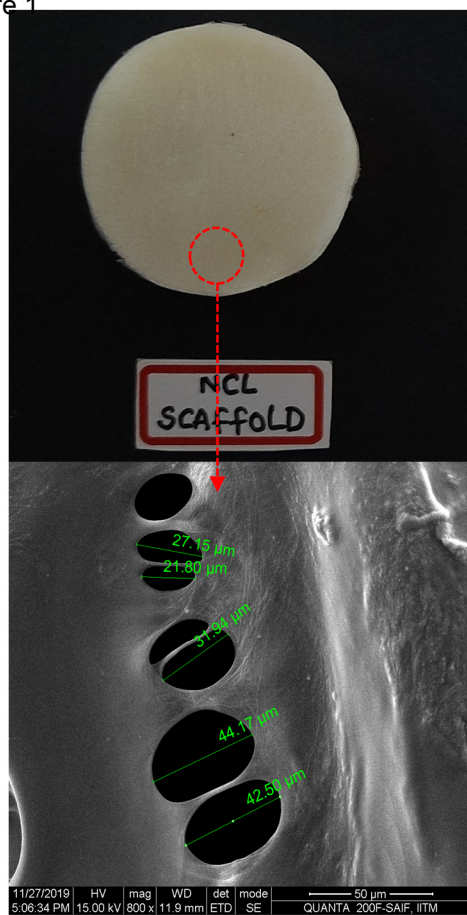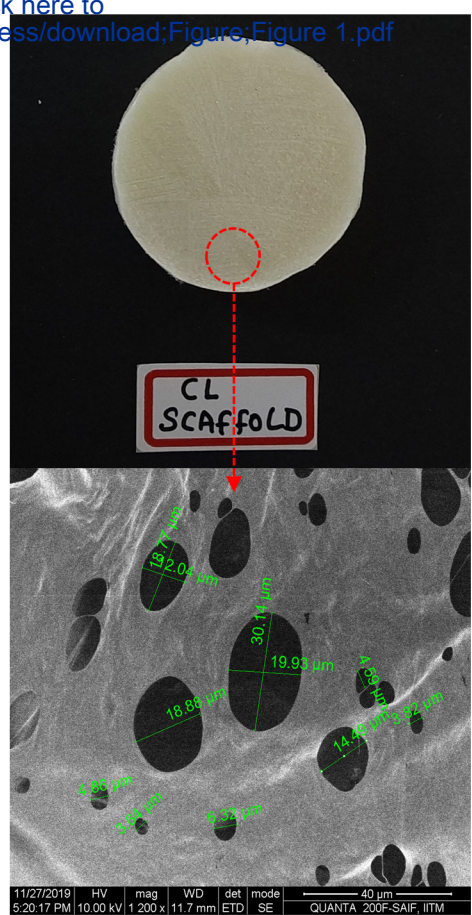
1b

Figure 2

Legend: DOX loaded NCL Scaffold ● ; DOX loaded CL Scaffold ■
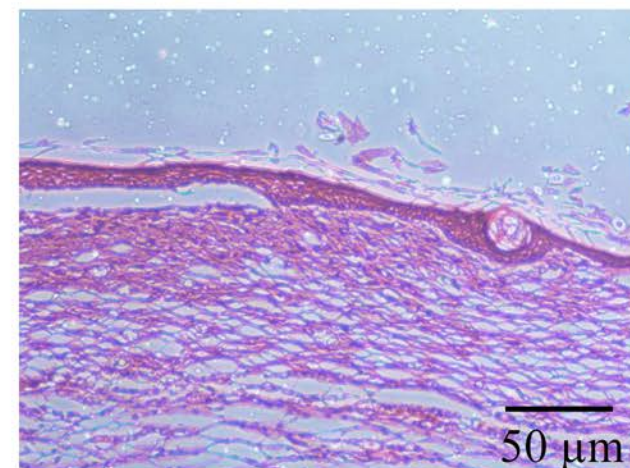
Figure 3

Legend: DOX loaded NCL Scaffold, DOX loaded CL Scaffold

Figure 4

Figure 5

5a

	Control	CL Scaffold	DOX-CL Scaffold
DAY 0			
DAY 7			
DAY 14			
DAY 21			

5b

Mean wound area in mm² vs Day
Control, CL Scaffold, DOX-CL Scaffold
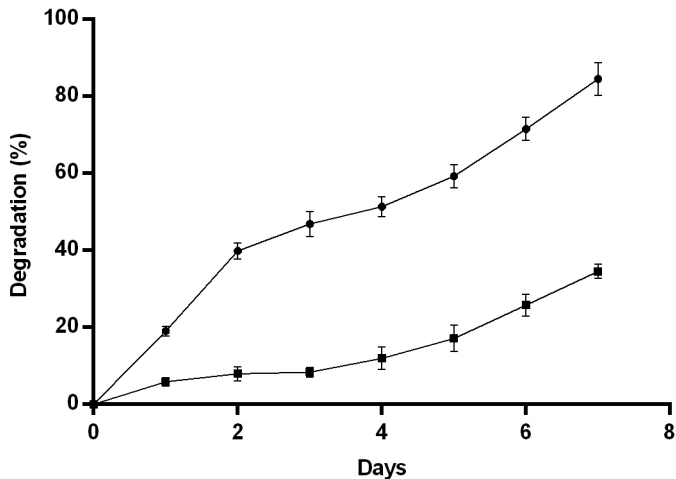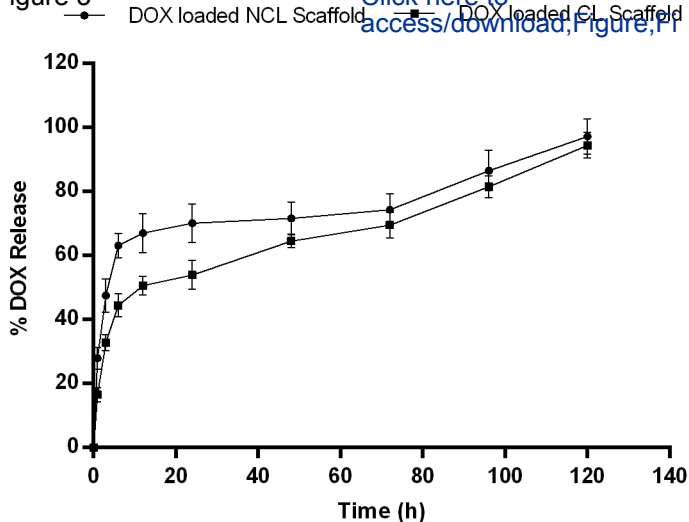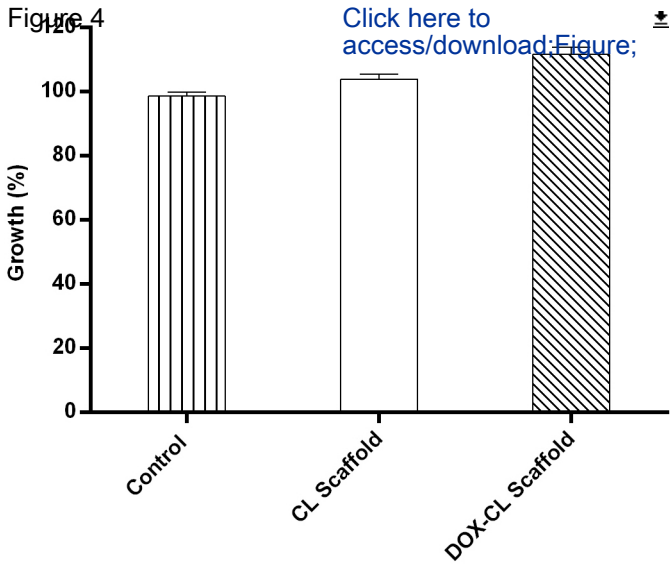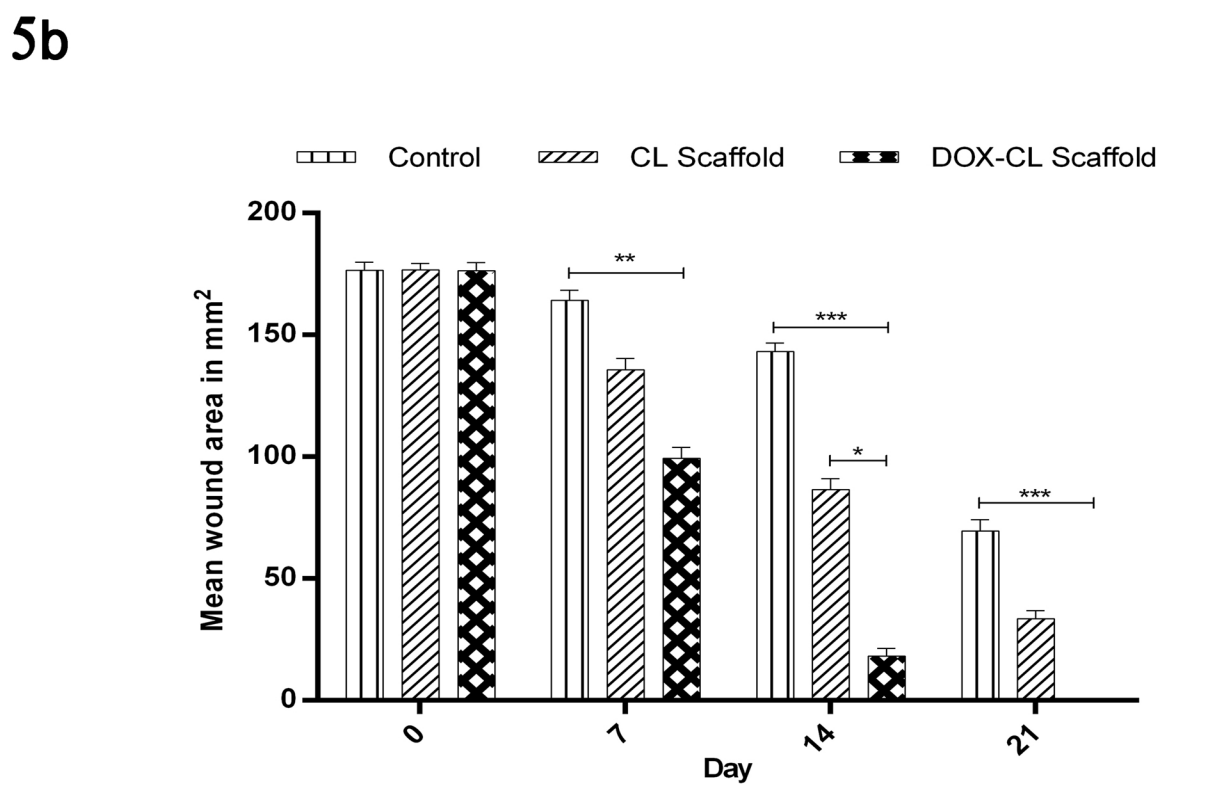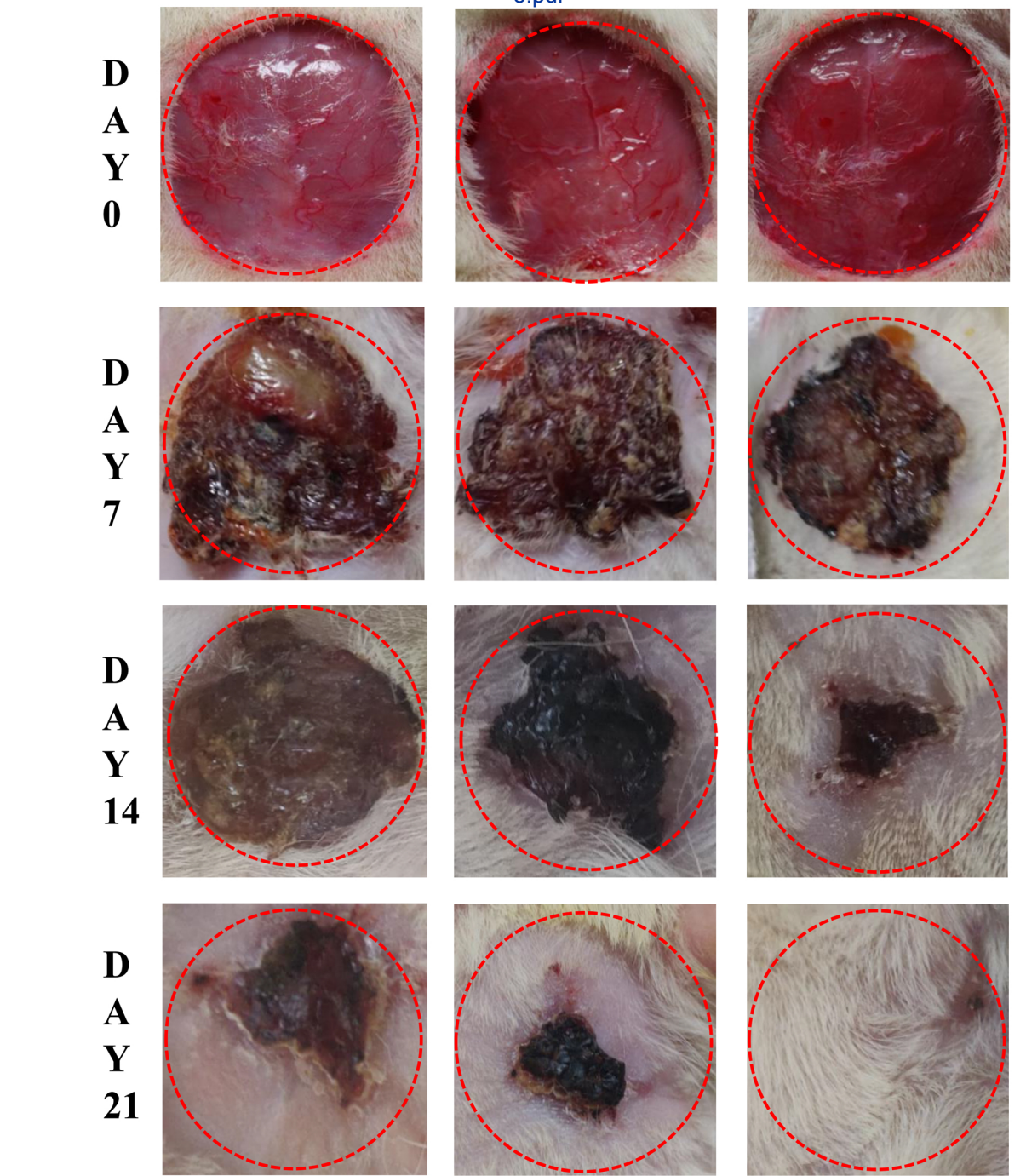
Figure 6

Control   **CL Scaffold**   **DOX-CL Scaffold**

DAY 7
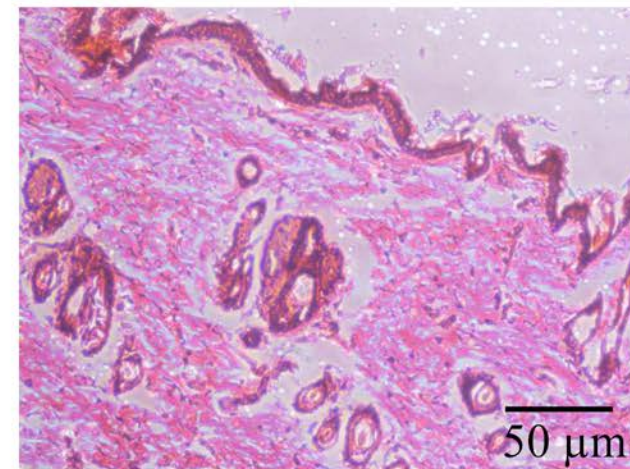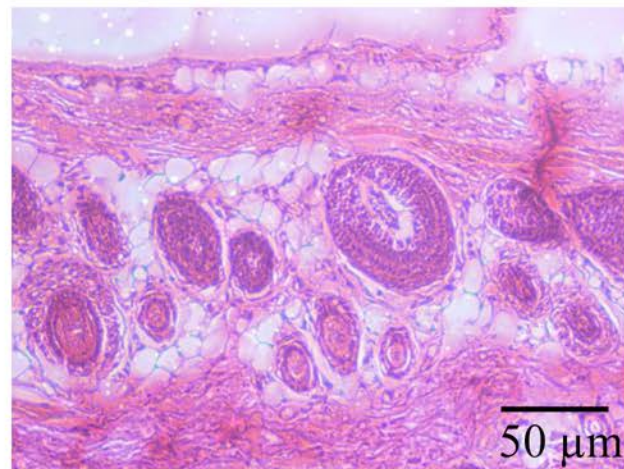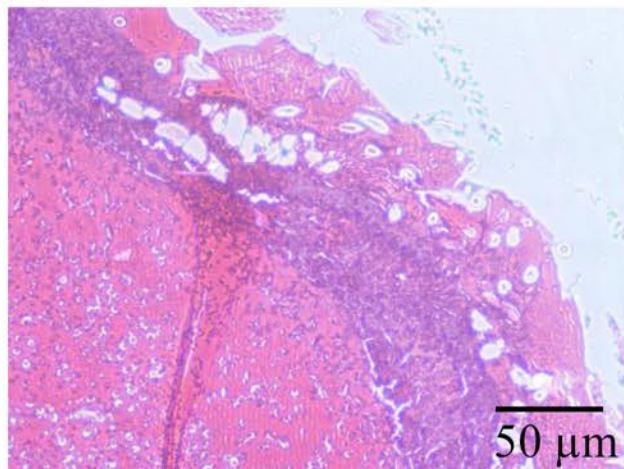
DAY 14
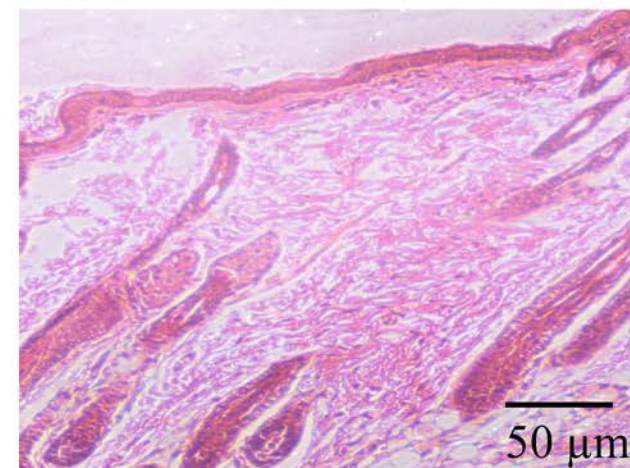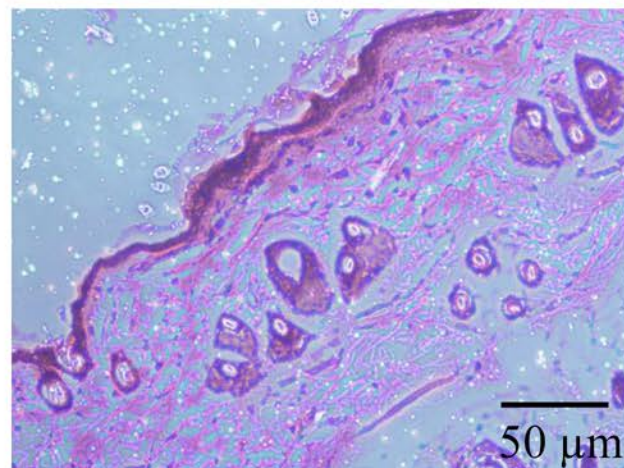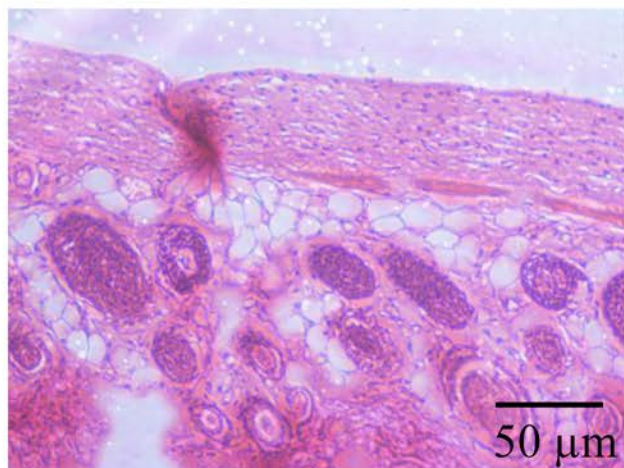
DAY 21
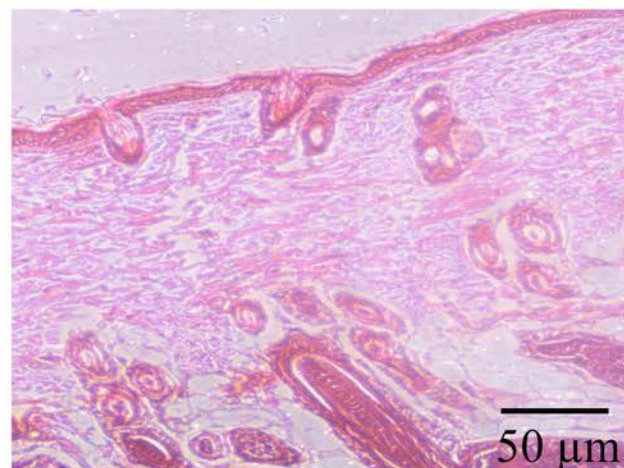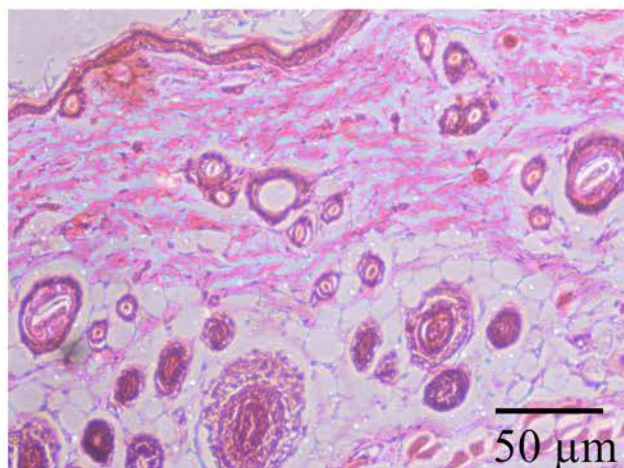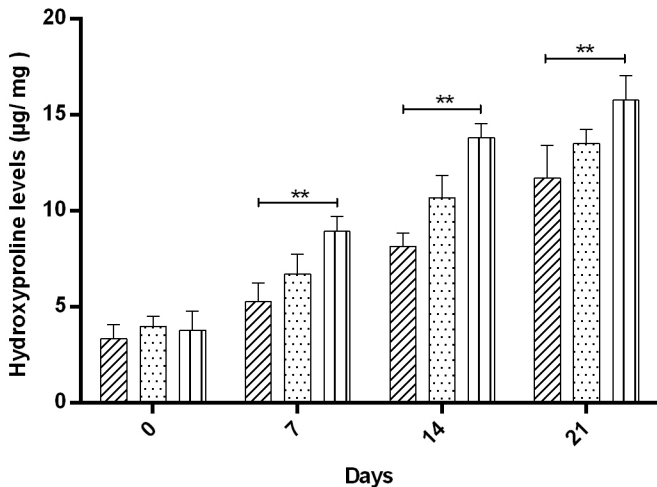
50 μm

Figure 7

Figure 8
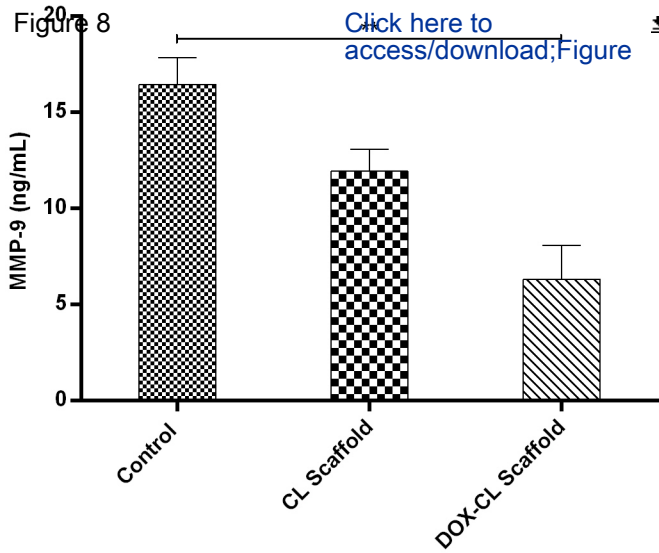
<div align="center">MIC (µg/mL)</div>

Test sample	*S. aureus*	*S. epidermis*	*E. coli*
DOX	<4	<4	<8
CS	<64	<64	<128
CL scaffold extract	<64	<64	<128
DOX-CL scaffold extract	<2	<2	<4

P. aeruginosa
<16
<128
<128
<4

Click here to access/download
Table of Materials
JoVE_Materials.xls

Cover Letter

Dr. Veera Venkata Satyanarayana Reddy. Karri

Assistant Professor

Department of Pharmaceutics

JSS College of Pharmacy, Ooty, India

20th May 2021

Dear editor,

Thank you for offering a thorough peer review. The comments shared were constructive and encouraging.

We have edited the video sections, and we hope that this will comply with the suggestions.

We want to thank the editor for their critical evaluation, valuable comments, and significant suggestions, which helped in improving the quality and clarity of this video.

Our responses and the corrections made (in blue) to each of the comments are listed below point by point:

Please find the attached rebuttal form

We believe that the revised video complies with editor comments, and we are very much interested in doing further revisions if necessary.

Sincerely,

Dr. Veera Venkata Satyanarayana Reddy. Karri

ksnreddy87@gmail.com

Title: Doxycycline Loaded Collagen/Chitosan Composite Scaffold for the Accelerated Healing of Diabetic Wounds (JoVE62184.R4)

Dear Editor,

Thank you for offering a thorough peer review. The comments shared were constructive and encouraging.

We have edited the video sections, and we hope that this will comply with the remarks.

We want to thank the Editor for their critical evaluation, valuable comments, and significant suggestions, which helped to improve the quality and clarity of this video.

The following are a list of corrections that were made in the original manuscript. Our responses and the corrections made (in blue) to each of the comments are listed below point by point:

Editorial comments:

Changes to be made by the Author(s) regarding the video:

1. Video & Audio Editing:

• **00:10-02:00 The audio levels in this range are still too loud. Please lower this volume by 3 dB (or around 10% of current levels).**
Response: As per the suggestion, we lowered the volume by 3 dB at 00:10-02:00 time

• **01:57 There seems to be an editing glitch here when he says "to accellerate the delayed healing in diabetic wounds" I think this part was accidently cut out in revision 1. Try restoring this sentence so it is not cut-up, creating the glitch.**
Response: We agree with the suggestion. We have now altered it to remove the glitch.